



BRILL

## WOOD DECAY BY *INONOTUS RICKII* AND *BJERKANDERA ADUSTA*: A MICRO- AND ULTRA-STRUCTURAL APPROACH

Carolina Analía Robles<sup>1,\*</sup>, María Agueda Castro<sup>2</sup> and Silvia Edith Lopez<sup>1</sup>

<sup>1</sup>PROPLAME-PRHIDEB-CONICET & <sup>2</sup>Laboratorio de Anatomía Vegetal Aplicada, Departamento de Biodiversidad y Biología Experimental, Facultad de Ciencias Exactas y Naturales, Universidad de Buenos Aires, Ciudad Universitaria, PB II, 4<sup>to</sup> piso, CP 1428EHA Ciudad Autónoma de Buenos Aires, Argentina

\*Corresponding author; e-mail: carorobles@bg.fcen.uba.ar

### ABSTRACT

*Bjerkandera adusta* (Willd.) P. Karst. and *Inonotus rickii* (Pat.) D. A. Reid. are important xylophagous fungi affecting street trees in Buenos Aires City, Argentina. The objective of this paper is to describe the decay patterns produced by these species in London plane wood (*Platanus acerifolia* (Ait.) Willd.), which is one of the most abundant tree species in the city, through light microscopy (LM), scanning electron microscopy (SEM) and transmission electron microscopy (TEM). A better knowledge of the decay patterns of these fungi at early stages would provide useful information for optimizing tree management programs. Microscopic observations showed that *B. adusta*, having caused an important loss of dry weight, showed more extensive degradation of wood after three months than *I. rickii*, affecting mainly fiber walls with potential consequences in tree strength and stiffness. *Inonotus rickii*, on the other hand, selectively affected vessel walls and middle lamellae between fibers. Rays remained virtually unaltered in all decayed wood.

**Keywords:** Wood-rotting fungi, white rot, delignification, *Platanus acerifolia*.

### INTRODUCTION

White-rot fungi remove lignin, cellulose and hemicelluloses from wood. Two main patterns are recognized. One is known as selective delignification, in which lignin is removed more than hemicelluloses or cellulose, at early stages of decay, and may be almost entirely removed in the secondary wall and middle lamellae (Levin & Castro 1998). Other decay fungi, instead, may break down lignin, cellulose and hemicelluloses at approximately the same rates. This is known as simultaneous white rot (Schwarze *et al.* 2000). During this process, the cells are left riddled with holes and erosion troughs or with extensively thinned secondary walls (Levin & Castro 1998).

The London plane tree (*Platanus acerifolia* (Ait.) Willd.) is one of the most frequent trees in cities. In Europe, it is used mainly in linear planting along streets, also in public and private parks and gardens (Tello *et al.* 2005). According to the last available data from the Government of Buenos Aires (Argentina), it is the second most frequent (Filipini *et al.* 2000) and one of the most affected by fungal decay (Sede & Lopez 1999).

In order to test the degradation ability of Basidiomycetes obtained from London plane trees, we have previously carried out a three-month *in vitro* study on *P. acerifolia* wood (Robles *et al.* 2011). Results showed that *Bjerkandera adusta* (Willd.) P. Karst. (Polyporales) caused the highest loss of dry weight (23.73 %) at the end of the assay and that *Inonotus rickii* (Pat.) D.A. Reid (Hymenochaetales) caused a loss of 8.45 % in dry weight during the same time (Robles *et al.* 2011). The latter, nevertheless, is considered one of the most harmful decay agents of urban trees, and has been reported in several cities of Europe and America, with a wide host range, a wide distribution and a high frequency of incidence (Melo *et al.* 2002; Annesi *et al.* 2003; Intini & Tello 2003; Robles *et al.* 2011).

*Bjerkandera adusta* has been reported both as a selective delignifier (Blanchette 1984) and as a simultaneous degrader (Anagnost 1998). Several species of *Inonotus*, such as *I. dryophilus* and *I. hispidus*, have been cited as selective delignifiers (Otjen & Blanchette 1982; Blanchette 1984; Otjen *et al.* 1987; Schwarze *et al.* 1995). Moreover, *I. hispidus* causes soft-rot cavities in *Fraxinus excelsior* (ash) and *Platanus acerifolia* wood (Schwarze *et al.* 1995). To our knowledge there are no previous studies on the decay patterns produced by *I. rickii*.

The aim of this work is to describe the main anatomical changes generated by *Bjerkandera adusta* and *Inonotus rickii* in London plane wood, using light microscopy (LM), scanning electron microscopy (SEM) and transmission electron microscopy (TEM). The latter technique was employed in order to assess the impact on the cellulose microfibrils pattern in vessels and fibers. A thorough knowledge of the decay patterns of these fungi would help to establish more accurate tree management programs, especially in urban environments.

## MATERIALS AND METHODS

*In vitro* weight losses of wood samples were determined according to the methodology used by Mielnichuk and Lopez (2007) and Robles *et al.* (2011). Blocks of about 1 × 3 × 0.5 cm of sound wood from branches of *Platanus acerifolia* were employed to estimate the degradation ability after three months of *Bjerkandera adusta* (BAFCcult 3301, BAFCcult: culture collection of the Facultad de Ciencias Exactas y Naturales, Universidad de Buenos Aires) and *Inonotus rickii* (BAFCcult 3300). Blocks were dried at 70 °C for 48h, then conditioned at 30 °C and weighed to determine the initial dry weight. Afterwards, each block was saturated by immersion in distilled water for 48 h and sterilized in an autoclave for 20 min at 105 kPa. MEA 1.25 % (Difco Lab.) slopes in 19 × 2 cm test tubes were inoculated with mycelial discs (about 0.6 diam.) of either one of the two decay species and then incubated at 25 °C. Once the mycelium covered the surface of the agar, one sterilized wood block was introduced into each test tube. Uninoculated wood blocks were used as controls. Nineteen replicates were arranged for each treatment. After 3 months of incubation in the dark at 25 °C, wood blocks were removed from the test tubes and the surface mycelium was gently cleaned off. Blocks were dried at 70 °C for 48 h, then at 30 °C and weighed to determine the final dry weight. Initial and final dry weights were used to calculate the weight loss caused by decay according to Mielnichuk and Lopez (2007).

Transverse sections, tangential longitudinal sections and radial longitudinal sections about 10–12  $\mu\text{m}$  thick were cut using a Leica microtome (SM2000R, Nussloch, Germany). For light microscopy studies, sections were double stained with safranin-fast green (Gurr BDH Chemicals, England), dehydrated in ethanol series (70% (v/v), 96% (v/v), 100% (v/v), 100% (v/v), 1–2 min each) and xylene (Berna, Argentina), and then mounted in synthetic balsam (PMYR, Instrumental Pasteur, Argentina). Transverse ultrathin sections (1  $\mu\text{m}$  thick) were stained on slides with 0.05% (w/v) toluidine blue (Merck Química Argentina S.A., Argentina) in 2.5% (w/v)  $\text{Na}_2\text{CO}_3$  solution (pH 11.1) at 60 °C for 1–6 min. Lignin autofluorescence and anisotropic cellulose properties were tested. In order to detect *pectin*, sections were treated with ruthenium red 0.01% (w/v) (Sigma Chemical, USA) (D'Ambrogio de Argüeso 1986).

Light microscopy (LM) observations were made using an UV Zeiss and Axioskop microscope (Oberkochen, Germany) equipped with an Olympus C-5060 Wide Zoom digital camera (Tokyo, Japan) and a Leica DM 2500 microscope (Wetzlar, Germany) equipped with a Leica EC3 digital camera (Heerbrugg, Switzerland).

For scanning electron microscopy (SEM) studies, sections about 12  $\mu\text{m}$  thick were dehydrated and examined in a Zeiss SUPRA TM 40 scanning electron microscope (Oberkochen, Germany).

For transmission electron microscopy (TEM), pieces of wood blocks of about 1  $\text{mm}^3$  were excised with a scalpel, fixed in 3% (v/v) glutaraldehyde in 0.2 M  $\text{Na}_2\text{HPO}_4$ – $\text{Na}_2\text{HPO}_4$  buffer solution (pH 7.4) at 4 °C for 12 h. Samples were then washed with the buffer for 24 h and postfixed in 1% (w/v)  $\text{OsO}_4$  aqueous solution at 20 °C for 2 h. Samples were washed with the same buffer for 1 h, dehydrated in an ascending ethanol series (50% (v/v), 70% (v/v), 90% (v/v), 100% (v/v), 15 min each) and an ethanol–acetone series (2:1, 2:2, 1:3; pure acetone, 15 min each) at 20 °C, and embedded in low viscosity Spurr's resin (Spurr 1969). Ultrathin sections (about 70 nm) were cut using a glass knife with a Sorvall MT-2B ultracut microtome (Newtown, USA), collected on copper grids and double stained with uranyl acetate and Reynolds lead-citrate (Reynolds 1963). Sections were examined using a Philips EM 301 transmission electron microscope (Eindhoven, Holland) at an accelerating voltage of 60 kV.

SEM and TEM observations were made at the Centro de Microscopías Avanzadas (Facultad de Ciencias Exactas y Naturales, Universidad de Buenos Aires).

## RESULTS

The observations under polarized light showed that *Bjerkandera adusta* caused a reduction of birefringence when compared to control wood. This was not observed in the wood affected by *Inonotus rickii*. A reduction of lignin autofluorescence was observed in all decayed wood when compared to the controls.

### *Light microscopy*

In transverse sections of control wood, vessel elements appeared solitary or grouped, polygonal to round and thick-walled; the axial parenchyma was scarce and diffuse whereas radial parenchyma cells were rectangular and radially elongated. All parenchyma cells exhibited cytoplasm, vacuoles and thick secondary walls. Fibers were

abundant, polygonal and very thick-walled. In general, with toluidine blue, the middle lamella stained dark blue and secondary walls purple blue (Fig. 1a).

In transverse sections, wood affected by *B. adusta* exhibited an evident heterogeneous intensity of the fungal attack (Fig. 1b–d). This species affected mainly the

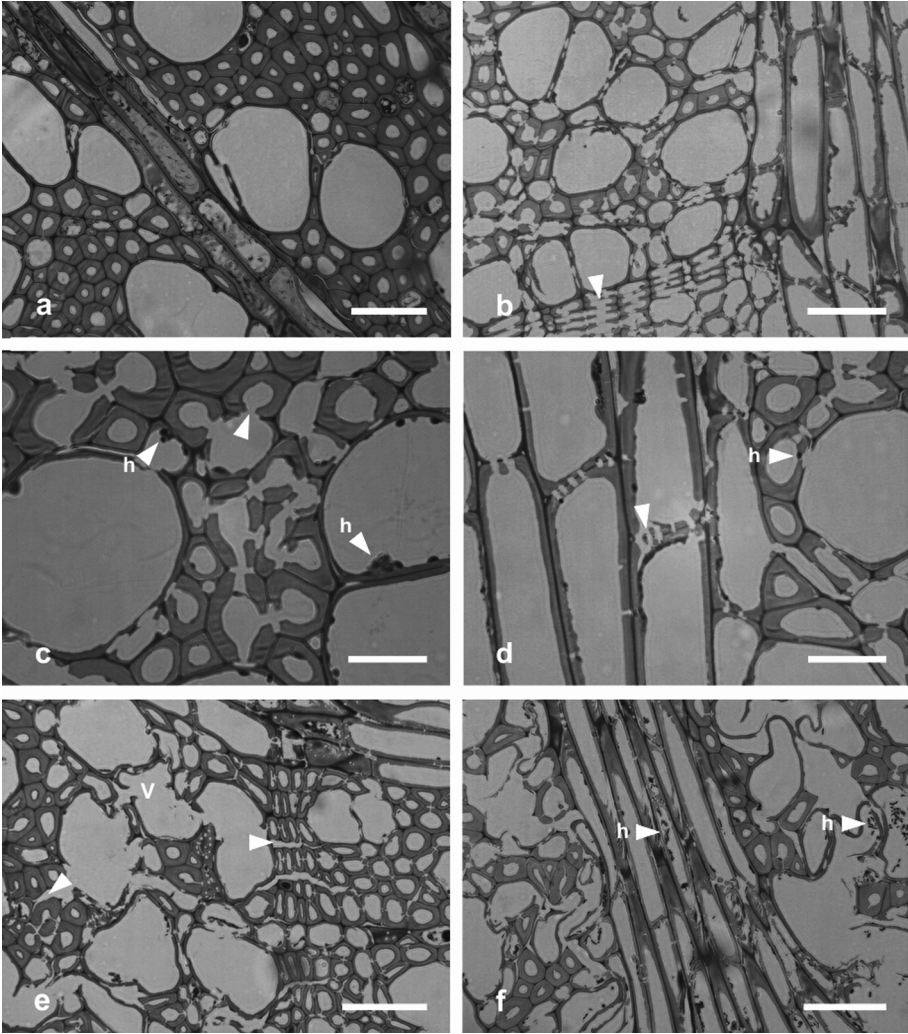


Figure 1. *Platanus acerifolia* wood decay. Transverse sections stained with toluidine blue, light micrographs. – a: Control block, general view. – b–d: *Bjerkandera adusta* decay. – b: Ray and growth ring boundary with broken tangential fiber walls (arrowhead) and terminal parenchyma. – c & d: Fiber-fiber and inter-parenchyma pit membrane collapse (arrowheads); pit cavity erosion, hyphae growing inside fibers and vessel elements. – e & f: *Inonotus rickii* decay. – e: Middle lamella absent between cells (arrowheads) in growth ring boundary, vessel elements with folded walls. – f: Abundant mycelia in vessel elements and rays. – h = hyphae; v = vessel element. – Scale bars = 50  $\mu\text{m}$  in a, b, e, f; 20  $\mu\text{m}$  in c, d.

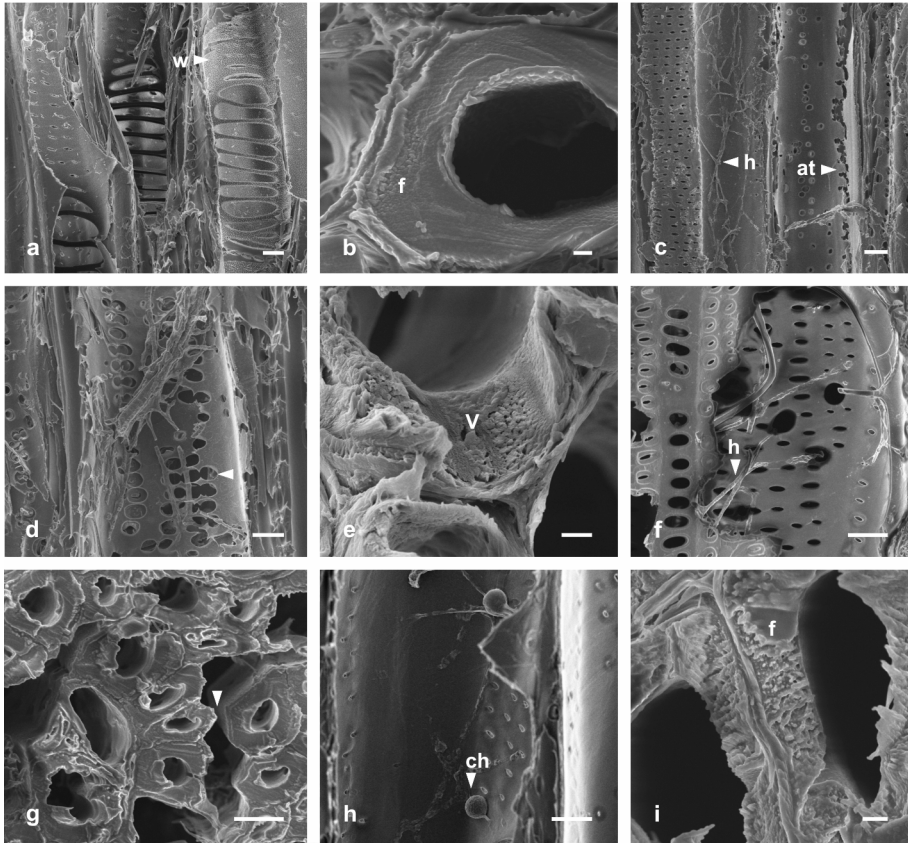


Figure 2. *Platanus acerifolia* wood decay, SEM micrographs. – a & b: Control block, longitudinal and transverse sections, respectively. – a: Vessel element with scalariform perforation plates and inner warty layer. – b: Fiber wall, detail. – c–e: *Bjerkandera adusta* decay. – c: Vessels with holes and axially elongated troughs. – d: Vessel wall collapse between pits (arrowhead). – e: Visible loosening and porosity of secondary vessel wall. – f–i: *Inonotus rickii* decay. – f: Hyphae growing through the eroded pit apertures. – g: Middle lamella collapse between fibers (arrowhead). – h: Chlamydospores in vessel element. – i: Fiber wall loosening and porosity. – at = axial troughs; f = fiber; h = hyphae; ch = chlamydospore; v = vessel element; w = warts. – Scale bars = 10  $\mu\text{m}$  in a, c, d, f–h; 1  $\mu\text{m}$  in b, e, i.

secondary walls of axial parenchyma and fibers. In distinct growth ring boundaries, tangential walls of fibers and terminal parenchyma appeared broken or with different degrees of degradation (Fig. 1b). Pit membranes were generally absent (Fig. 1c, d). Vessel elements were less affected than fibers and similar to those in control wood. Rays remained structured (Fig. 1b, d). Axial and radial parenchyma appeared empty, suggesting collapsed membranes. Hyphae were inside the lumen of vessels, fibers and parenchyma cells, in contact with their inner walls and growing from cell to cell through pits. Conspicuous erosion of pit cavities was observed (Fig. 1c, d).

In wood affected by *I. rickii*, evident degradation of middle lamellae between cells occurred mainly at the level of growth ring boundaries and less accentuated between fibers in growth rings (Fig. 1e). In general, the secondary wall of vessels appeared collapsed, thin, folded and/or broken (Fig. 1e, f). In the proximity of degraded vessel elements, pockets of fibers and axial parenchyma were partially destroyed or absent. Rays remained unaffected (Fig. 1f). Most of axial and radial parenchyma cells appeared empty, suggesting collapsed membranes. Mycelia were abundant in vessel elements and rays (Fig. 1f).

### **Scanning electron microscopy**

In control wood, vessel elements showed both simple and scalariform perforation plates and a warty inner layer (Fig. 2a). In fibers, and axial and radial parenchyma, walls appeared thick and entire (Fig. 2b).

In wood affected by *B. adusta*, the vessel elements presented a smooth inner surface of secondary walls, suggesting the complete degradation of warts (Fig. 2a, c). Outer vessel walls showed holes, axially elongated troughs alongside the growing hyphae (Fig. 2c), and coalescent pits (Fig. 2d). After three months, the progressive delignification caused visible loosening and porosity of secondary vessel walls (Fig. 2e).

In wood affected by *I. rickii*, decay caused degradation of warty layers of vessels, collapse of the pit membrane and an increase in pit aperture size (Fig. 2a, f). Complete degradation of the middle lamella was observed between fibers (Fig. 2g). Chlamydospores were detected in vessel elements and rays (Fig. 2h). Signs of fiber wall looseness were observed (Fig. 2i).

### **Transmission electron microscopy**

In control wood, the compound middle lamella between vessels, axial and radial parenchyma and fibers appeared electronically dense. In all cases, secondary walls showed the characteristic pattern of cellulose microfibrils, exhibiting a warty inner layer only in vessels and fibers (Fig. 3a–c). Fiber secondary walls showed three distinct layers: S<sub>1</sub>, S<sub>2</sub> and S<sub>3</sub> (Fig. 3c). S<sub>1</sub> and S<sub>3</sub> were slightly electronically denser than the thickest S<sub>2</sub>.

In wood affected by *B. adusta*, vessel element walls showed a heterogeneous electron-dense pattern. Secondary walls in contact with hyphae appeared translucent with several electron-dense patches. Lignin degradation (confirmed by lignin autofluorescence) caused a loose arrangement of cellulose microfibrils. The middle lamella was electron-dense (Fig. 3d). Localized wall degradation, causing irregular to elongate translucent troughs, was observed in radial parenchyma cells (Fig. 3e). Fiber secondary walls did not show the typical S<sub>1</sub>, S<sub>2</sub> and S<sub>3</sub> layers; in general, layers were less dense than the control. When in contact with hyphae, concentric lamellae with different density were recognized (Fig. 3f).

In wood affected by *I. rickii*, vessel secondary walls were electronically denser than those from wood affected by *B. adusta*. A narrow electron-dense band, extended and discontinuous, was distinguished next to hyphae (Fig. 3g). Axial parenchyma secondary walls revealed the presence of irregular electron-dense areas intermixed with trans-

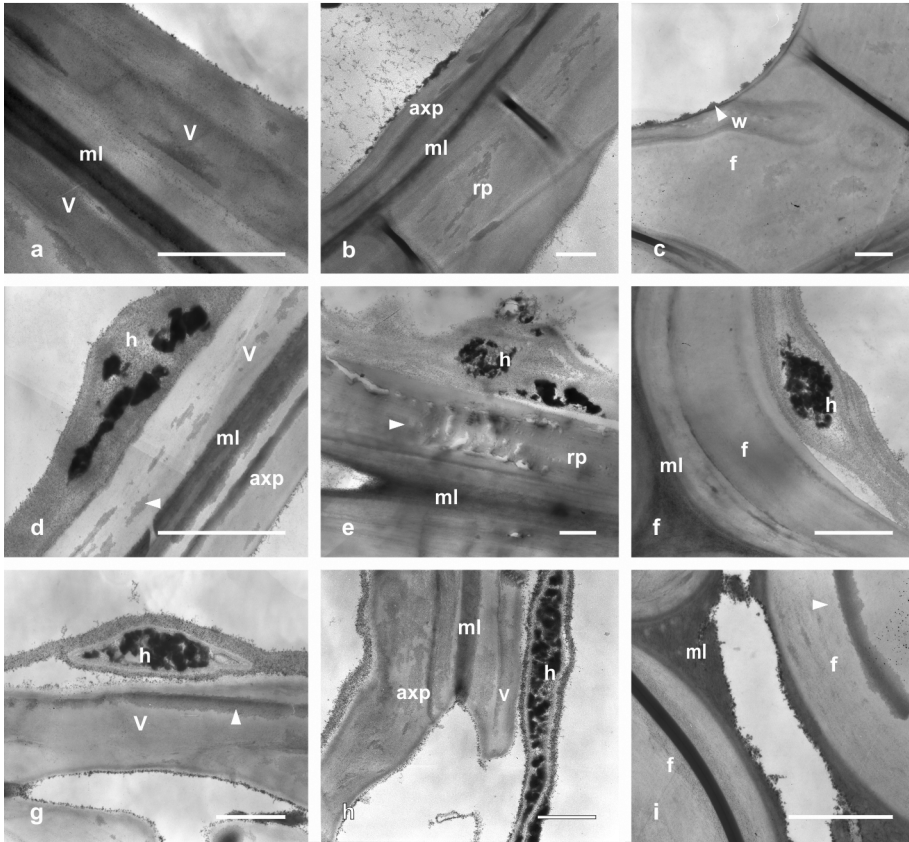


Figure 3. *Platanus acerifolia* wood decay. TEM micrographs. – a–c: Wall details in control block. – a: Vessel elements. – b: Axial and radial parenchyma. – c: Fiber. – d–f: *Bjerkandera adusta* decay. – d: Vessel wall with a heterogeneous electron density pattern (arrowhead). – e: Ray wall alteration (arrowhead). – f: Fiber wall layers with different densities. – g–i: *Inonotus rickii* decay. – g: Vessel wall with a narrow electron-dense band near the hyphae (arrowhead). – h: Axial parenchyma wall with heterogeneous density pattern. – i: Fiber wall with an electron-dense band (arrowhead) and partial middle lamella collapse. axp = axial parenchyma; f = fiber; h = hyphae; ml = middle lamella; rp = radial parenchyma; v = vessel element; w = wart. — Scale bars = 1  $\mu\text{m}$ .

lucent spots (Fig. 3h). The secondary walls of fibers presented electron-dense bands intermixed with thick and translucent ones. Lignin degradation of the middle lamella caused separation between fibers (Fig. 3i).

#### DISCUSSION AND CONCLUSIONS

This is an extensive description involving a microscopic and ultrastructural approach of the decay pattern caused by *Bjerkandera adusta* and by *Inonotus rickii*. Light and

electron microscopy showed the main cell wall alterations and two different patterns of white-rot in London plane wood at early stages of decay.

*Inonotus rickii* exhibited a selective delignification pattern which caused conspicuous loss of lignin in the middle lamellae between fibers and attack of the vessel walls. In contrast, *Bjerkandera adusta* displayed a more severe wood decay, affecting mainly fiber walls, reducing rigidity and strength.

Vessels are recognized as extremely resistant to attack by some white-rot fungi. It is known that high concentrations of lignin in vessel walls, differences in the arrangement of lignin in the wall layers, and lignin monomer composition are some of the main cited factors that contribute to the integrity of vessels after fungal attack. In general, vessels have a greater guaiacyl/syringyl units ratio than other cells (Blanchette *et al.* 1987; Nilsson & Daniel 1989) and guaiacyl lignin seems to be more difficult to degrade than syringyl lignin (Blanchette *et al.* 1990). In poplar wood decayed by *Trametes trogii*, *Pycnoporus sanguineus* and *Ganoderma lucidum*, Levin and Castro (1998) and Luna *et al.* (2004) observed that vessels were the most resistant cells. Preferential degradation of vessel walls by *I. rickii* and their structural integrity in wood affected by *B. adusta* indicate that the enzymatic system of these species differs in their action on lignin. Further investigations are needed to confirm this hypothesis. Several enzymes involved in lignin degradation, as LiP (lignin peroxidase), MnP (manganese peroxidase) and VP (versatile peroxidase) have been detected in *B. adusta* (Ward *et al.* 2004). The enzymatic system of *I. rickii* has not yet been studied in detail.

In both decays, rays remained apparently unaffected. The fungi grew centripetally through rays and axially (to top and base) throughout the lumen of vessels and fibers. This supports the hypothesis that the radial system acts as an effective and quick pathway for colonization and access to the axial system. Schwarze and Fink (1997) noted the resistance of London plane xylem rays to degradation by *I. hispidus* and suggested that this could be associated with the formation of polyphenolic deposits in the lumina of cells or within the intercellular spaces between adjacent xylem ray cells. However, these deposits were not observed in the present *in vitro* assays.

In general, hyphae were observed in the lumen of cells growing in contact to the inner surface cell walls and crossing cell to cell throughout pits. This is the most frequent form of colonization of wood by hyphae (Schwarze 2007).

The results obtained from histochemical essays were consistent with LM, SEM and TEM observations. Changes in birefringence caused by *B. adusta* indicate cellulose disorganization involving loss of crystallinity. This could be consistent with a simultaneous type of decay.

Chlamydo spores are thick-walled resting spores which survive unfavorable conditions. They are produced by *I. rickii* in both basidioma and culture (Wright & Iaconis 1955). The chlamydo spores observed in wood inoculated with this species suggest its major potential of spread and high capacity of new host's colonization. This qualifies *I. rickii* as a species to consider, although it does not cause a high loss of dry weight in wood at early stages of decay. *Bjerkandera adusta*, on the other hand, did not produce any propagules in the wood as it usually does in culture (Stalpers 1978). This suggests a lower spread capacity than that of *I. rickii*.

In relation to the decay pattern, there are several reports of species of *Inonotus*, such as *I. dryophilus* and *I. ludovicianus* in *Quercus* and *Betula papyrifera*, *I. rheades* in *Populus* sp., *I. texanus* in *Prosopis* sp., *I. tomentosus* in *Picea glauca* (Otjen & Blanchette 1982; Blanchette 1984; Otjen *et al.* 1987), which cause selective delignification on wood, removing the middle lamella and causing separation between cells (Blanchette 1984). Schwarze *et al.* (1995) observed that *Inonotus hispidus* produced a selective delignification in ash wood, with degradation initiating in the corners of the middle lamellae within the xylem rays without pronounced effect on the primary and secondary wall layers. This species caused also soft-rot cavities (type-1 soft-rot attack) in both ash and London plane wood. Simultaneous rot caused by *Inonotus* (*I. hispidus*) has also been reported (Schubert *et al.* 2008). To our knowledge, there are no studies focused on *I. rickii* decay patterns. In London plane wood this species would act as a selective delignifier at early stages of decay.

On the other hand, there are contradictory reports of the decay caused by *B. adusta*. Blanchette (1984) observed that this fungus caused a selective delignification in *Betula papyrifera*, selectively removed middle lamella and defibrated cells. This was corroborated by chemical analysis of percentages of lignin, cellulose, mannose and xylose. Anagnost (1998) reported that *B. adusta* caused a simultaneous rot in yellow birch (*Betula alleghaniensis* Britton) producing lumen and pit erosion. Our results regarding *B. adusta* decay pattern are more similar to Anagnost's observations.

The present paper is the first extensive and comparative study involving both decay fungi at the structural micro- and ultra-structural level. Although *in vitro* assays cannot be taken as absolute evidence of the behavior of xylophagous fungi, they are a useful tool to analyze wood decay patterns. At early stages of decay *B. adusta* would mainly alter wood strength and stiffness, unlike *I. rickii*. The knowledge of the main structural decay features would help to define the level of risk in early stages and optimize decisions related to management of urban trees in each case.

#### ACKNOWLEDGEMENTS

This work was supported by CONICET PIP 1482, and Universidad de Buenos Aires, Argentina UBA-CYT X122. Publication number 192 PRHIDEB CONICET.

#### REFERENCES

- Anagnost SE. 1998. Light microscopy diagnosis of wood decay. IAWA J. 19: 141–167.
- Annesi T, Coppola R & Motta E. 2003. Decay and canker caused by *Inonotus rickii* spreading on more urban tree species. Forest Pathol. 33: 405–412.
- Blanchette RA. 1984. Screening wood decayed by white rot fungi for preferential lignin degradation. Appl. Environ. Microbiol. 48: 647–653.
- Blanchette RA, Abad A, Nilsson T & Daniel D. 1990. Biological degradation of wood. Adv. Chem. Ser. 225: 141–174.
- Blanchette RA, Obst JR, Hedges JI & Weliky K. 1987. Resistance of hardwood vessels to degradation by white rot basidiomycetes. Can. J. Bot. 66: 1841–1847.
- D'Ambrogio de Argüeso A. 1986. Manual de técnicas en histología vegetal. Hemisferio Sur, Buenos Aires.

- Filippini LM, Bustillo L, Moruzzi HP, Inomata F, Florentino JA & Laudani AM. 2000. El Arbolado de la Ciudad de Buenos Aires. Santísima Trinidad, Buenos Aires.
- Intini M & Tello ML. 2003. Investigaciones sobre hongos xilófagos de árboles urbanos en Europa: primera cita de *Inonotus rickii* (Pa.) Reid en España. Bol. Sanid. Veg. Plagas 29: 277–279.
- Levin L & Castro MA. 1998. Anatomical study of the decay caused by the white-rot fungus *Trametes trogii* (Aphyllphorales) in wood of *Salix* and *Populus*. IAWA J. 19: 169–180.
- Luna ML, Murace MA, Keil GD & Otaño ME. 2004. Patterns of decay caused by *Pycnoporus sanguineus* and *Ganoderma lucidum* (Aphyllphorales) in poplar wood. IAWA J. 25: 425–433.
- Melo I, Ramos P & Caetano MFF. 2002. First record of *Inonotus rickii* (Basidiomycetes, Hymenochaetaceae) in Portugal. Portugaliae Acta. Biol. 20: 265–269.
- Mielnichuk N & Lopez SE. 2007. Interaction between *Epicoccum purpurascens* and xylophagous basidiomycetes on wood blocks. Forest Pathol. 37: 236–242.
- Nilsson T & Daniel G. 1989. Chemistry and microscopy of wood decay by some higher Ascomycetes. Holzforschung 43: 11–18.
- Otjen L & Blanchette RA. 1982. Patterns of decay caused by *Inonotus dryophilus* (Aphyllphorales: Hymenochaetaceae), a white pocket rot fungus of oaks. Can. J. Bot. 60: 2270–2279.
- Otjen L, Blanchette R, Effland M & Leathan G. 1987. Assessment of 30 white rot basidiomycetes for selective lignin degradation. Holzforschung 41: 343–349.
- Reynolds ES. 1963. The use of lead citrate at high pH as an electron opaque stain in electron microscopy. J. Cell Biol. 17: 208–212.
- Robles CA, Carmarán CC & Lopez SE. 2011. Screening of xylophagous fungi associated with *Platanus acerifolia* in urban landscapes: Biodiversity and potential biodeterioration. Landscape Urban Plan. 100: 129–135.
- Schubert M, Fink S & Schwarze FWMR. 2008. Evaluation of *Trichoderma* spp. as a biocontrol agent against wood decay fungi in urban trees. Biol. Control 45: 111–123.
- Schwarze FWMR. 2007. Wood decay under the microscope. Fungal Biol. Rev. 21: 133–170.
- Schwarze FWMR, Engels J & Mattheck C. 2000. Fungal strategies of wood decay in trees. Springer, New York.
- Schwarze FWMR & Fink S. 1997. Reaction zone penetration and prolonged persistence of xylem rays in London plane wood degraded by the basidiomycete *Inonotus hispidus*. Mycol. Res. 101: 1207–1214.
- Schwarze FWMR, Lonsdale D & Fink S. 1995. Soft rot and multiple T-branching by the basidiomycete *Inonotus hispidus* in ash and London plane. Mycol. Res. 99: 813–820.
- Sede SM & Lopez SE. 1999. Xylophagous fungi of urban trees in Buenos Aires City. Mycologist 13: 173–175.
- Spurr AR. 1969. A low-viscosity epoxy resin embedding medium for electron microscopy. J. Ultrastruct. Res. 26: 31–43.
- Stalpers JA. 1978. Identification of wood-inhabiting fungi in pure culture. Stud. Mycol. 16: 1–248.
- Tello ML, Redondo C, Gaforio L, Pastor S & Sagasta EM. 2005. Development of a disease severity rating scale for plane tree anthracnose. Urban For. & Urban Green. 3: 93–101.
- Ward G, Hadar Y & Dosoretz CG. 2004. The biodegradation of lignocelluloses by white rot fungi. In: Arora DK (ed.), Fungal biotechnology in agricultural food, and environmental applications: 393–407. Marcel Dekker, New York.
- Wright JE & Iaconis CL. 1955. Estudios sobre Basidiomycetes III. “*Polyporus rickii*” f. sp. “*negundis*” sobre arces vivos. Rev. Invest. Agric. 9: 97–109.

Accepted: 9 January 2013

Associate Editor: Susan Anagnost